Bioorganic & Medicinal Chemistry 20 (2012) 207–214

Contents lists available at SciVerse ScienceDirect

Bioorganic & Medicinal Chemistry

journal homepage: www.elsevier.com/locate/bmc

Conjugation of a 3-(1*H*-phenanthro[9,10-*d*]imidazol-2-yl)-1*H*-indole intercalator to a triplex oligonucleotide and to a three-way junction

Maha I. Fatthalla [a,b], Yehya M. Elkholy [b], Nermeen S. Abbas [b], Adel H. Mandour [c], Per T. Jørgensen [a], Niels Bomholt [a], Erik B. Pedersen [a,*]

[a] *Nucleic Acid Center, Department of Physics, Chemistry and Pharmacy, University of Southern Denmark, Campusvej 55, 5230 Odense M, Denmark*
[b] *Department of Chemistry, Faculty of Science, Helwan University, 11795 Ain Helwan, Cairo, Egypt*
[c] *Natural Product Chemistry, National Research Center, Dokki, Egypt*

ARTICLE INFO

Article history:
Received 15 July 2011
Revised 2 November 2011
Accepted 7 November 2011
Available online 13 November 2011

Keywords:
Indole
Triplex Forming Oligonucleotide
Three-way junction
Thermal stability
Fluorescence
Molecular modeling

ABSTRACT

A new intercalating nucleic acid monomer **M** comprising a 4-(1-indole)-butane-1,2-diol moiety was synthesized via a classical alkylation reaction of indole-3-carboxaldehyde followed by a condensation reaction with phenanthrene-9,10-dione in the presence of ammonium acetate to form a phenanthroimidazole moiety linked to the indole ring. Insertion of the new intercalator as a bulge into a Triplex Forming Oligonucleotide resulted in good thermal stability of the corresponding Hoogsteen-type triplexes. Molecular modeling supports the possible intercalating ability of **M**. Hybridisation properties of DNA/DNA and RNA/DNA three-way junctions (TWJ) with **M** in the branching point were also evaluated by their thermal stability at pH 7. DNA/DNA TWJ showed increase in thermal stability compared to wild type oligonucleotides whereas this was not the case for RNA/DNA TWJ.

1. Introduction

Secondary structure formation, including triple helix, is one of the extraordinary properties that nucleic acid adopts. The third oligonucleotide strand was first described by Felsenfeld and Rich,[1] referred to as the Triplex Forming Oligonucleotide (TFO). The triplex can be formed if the targeted strand is rich in purines, which in addition to the bonds of the Watson–Crick base pairing can form two further hydrogen bonds, Hoogsteen or reverse Hoogsteen, able to bind with a third matching oligonucleotide strand.[2] As the human genome often contains sequences rich in purines,[3] specific duplex DNA targeting by TFO provides an attractive strategy to induce genetic manipulation by homologous exchange using single-stranded oligodeoxynucleosides with the ultimate goal of repairing genetic defects (site-directed mutagenesis, site-directed recombination, etc.) in human cells.[4,5] Duplex DNA targeted by TFO has also been reported for regulating the expression of genes that are responsible for the synthesis of protein(s)/enzyme(s) for specific diseases by locking their transcription (antigene).[6] In this context TFO could be used to deliver drugs to a specific site in the genome[7] and to direct validated anticancer drugs to genes carrying cancer-specific mutations or translocations thereby inducing DNA damage selectively to tumor cells.[8] Fully phosphorothioate 25-mer antiparallel TFO shows significant results to attenuate liver fibrosis.[9] Interestingly, the TFOs were also used in antigene radiotherapy,[10] for example treating psoriasis and other inflammatory or malignant skin diseases by psoralen conjugated to TFO.[11] Also intercellular gene targeting, identification of genes that is responsible for the cell growth and malignant transformation,[12] TFO helps to study the molecular mechanism of enzymes by interfering binding with polymerase[13] endonuclease[14] and methylase[15] enzymes, to label DNA site-specifically and to purify and recognize DNA.[16] Circular TFOs are of particular interest, since these are not substrates for degradation by exonucleases.[17]

Junctions in nucleic acid structures are formed when three or more helices meet at a single point. These branched junctions are important intermediates in many biological functions and play important roles in many cellular processes.[18] Three-way junctions (TWJs) are the simplest type of junctions and consist of three double helical arms connected at the junction point. TWJs are formed both in DNA and RNA. In RNA, they are involved in splicing[19] and translation,[20] while in DNA, they are formed transiently during DNA replication (the replication fork[21]) and during recombination involving phages.[22] Furthermore, DNA-TWJs were proposed to occur in the triplet repeats expansions found in genetically unstable genomic DNA associated with human diseases such as Huntington's.[23] Beside their roles in biological processes, branched

* Corresponding author. Tel.: +45 65502555; fax: +45 66158780.
E-mail address: ebp@ifk.sdu.dk (E.B. Pedersen).

0968-0896/$ - see front matter © 2011 Elsevier Ltd. All rights reserved.
doi:10.1016/j.bmc.2011.11.013

junctions offer a unique window into DNA nanotechnology, which includes the controlled self-assembly of nanometer-scale molecular fragments.[24] Because TWJs are the smallest type of junction structures, they are used as a model system to gain insight into other complex and multi-branched junction structures, such as the Holliday junction, which is a key intermediate in homologous recombination. TWJs, therefore, provide a suitable system for assessing the quantitative features of junction structures.[25]

Triplexes are thermodynamically less stable than the corresponding duplexes at neutral pH because protonation of cytosine is providing stable Hoogsteen base pairing in pyrimidine triplexes.[26] This poor stability limits its applicability in vitro and in vivo.[27] To overcome this limitation, many trials have been made to increase binding ability either in the major or minor grooves of the duplex. Developing TFOs that have chemically modified nucleotides that bind in the major groove region such as locked nucleic acid (LNA),[28] peptide nucleic acid (PNA),[29] or bulge insertion of heterocyclic compounds (intercalators)[30] proofed its efficiency to increase the affinity of the TFO for specific target sequences and to stabilize the corresponding triplexes.[31] Also some small compounds like aminoglycosides[32] and some polyhydroxylated compounds[33] function as DNA minor groove binding ligands. Addition of metal ion as nanoparticles have been recently reported.[34] Our interest is to develop new intercalating moieties for bulge insertion in the TFO. It is believed that the intercalator design being able to stabilize the TFO via intercalation and stacking in Hoogsteen-type helixes should contain a long and large conjugated aromatic surface enough to place the intercalator into the dsDNA part of the triple helix together with a short flexible linker to the sugar–phosphate backbone to minimize the entropy effect.[35]

Recently, we have reported the synthesis and properties of intercalating nucleic acids designed for Hoogsteen-type triplexes with bulge insertions of aromatic moieties into the middle of homopyrimidine oligonucleotide (ON). An extraordinary high thermal stability was found for the corresponding triplexes. The pyrene dependant, (*R*)-1-*O*-[4-(1-pyrenylethynyl)phenylmeth-yl]glycerol (**W**, twisted intercalating nucleic acid, TINA, Fig. 1)[36] and the phenanthrene dependant monomers (*S*)-4-(4-(1*H*-phenanthro[9,10-*d*]imidazol-2-yl)-phenoxy)butane-1,2-diol (**X**) and (*S*)-4-(4-(1*H*-phenanthro[9,10-*d*]imidazol-2-yl)naphalen-1-yloxy)butane-1,2-diol (**Y**). In the latter molecule, the phenyl group in **X** has been replaced by a naphthyl group hoping to get better stacking ability (Fig. 1). However, a decrease in the thermal stability of **Y** was reported compared to **W** and **X** which was explained by sterical clashes between protons on the naphthalene and the imidazole moieties forcing the naphthalene ring out of planarity.[37]

In the present work we decided to make some more modification on the **X** monomer design in order to minimize sterical clashes between the two ring systems. Therefore, we replaced the naphthalene ring in the monomer **Y** with an indole ring system that has different spatial arrangement. The new synthesized monomer **M** was inserted into a 14-mer homopyrimidine oligonucleotide for thermal triplex stability studies and this proved enhanced triplex stability compared to wild type. In addition, DNA and RNA TWJs hybridisation stabilities were also studied by introducing monomer **M** into the junction region as a bulge. It is worth to note that we are the first to use an indole ring as an intercalating oligonucleotide system. Indoles have previously been used as artificial DNA bases in oligonucleotides.[38]

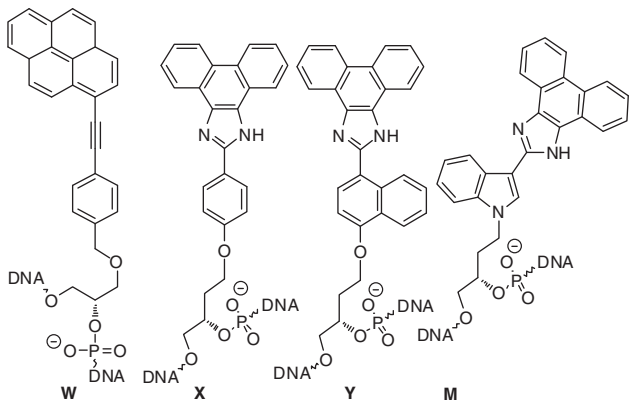

Figure 1. Structure of intercalators **M**, **W**, **X** and **Y**.

2. Chemistry

The intercalating nucleic acid monomer **9** was synthesized as described in Scheme 1. N-Alkylation of indole-3-carboxaldehyde is a key step in order to accomplish linking of the intercalating moiety to a backbone monomer. Many trials were made using a dioxolane ethanol as an alkylating agent to get a high yield of N-alkylated indole-3-carboxaldehyde **4**. Ruthenium-catalyzed alkylation,[39] Mitsunobu reaction[40] and microwave assisted reaction[41] all failed to get the product in a higher yield than 20%. Also in another strategy by formylation of the N-alkylated indole,[42] we failed and got the starting material as the sole product. It was more successful to use the classical method that involve treatment of the commercially available indole-3-carboxaldehyde **3** with NaH as a base together with triethyl amine using the dioxolane mesylate **2** as the alkylating reagent in dry DMF.[43] Hydrochloric acid was subsequently added to cleave the isopropylidene protection group to get the diol **4** in 49% overall yield. Treatment of **4** with phenanthrene-9,10-dione **5** and ammonium acetate in hot glacial acetic acid[44] afforded the diacetylated monomer **6** in 76% yield instead of the expected diol monomer **7**. The latter was obtained in 78% yield as a solid compound by subsequent treatment of the diacetylated compound **6** with saturated methanolic ammonia.[45] The primary hydroxy group was protected by reaction with 4,4′-dimethoxytrityl chloride (DMTCl) in anhydrous pyridine containing triethyl amine[46] at room temperature under a N_2 atmosphere. Silica gel chromatography afforded the DMT-protected compound **8** in 85% yield. The secondary hydroxy group was phosphitylated overnight with 2-cyanoethyl *N*,*N*,*N*′,*N*′-tetraisopropyl phosphorodiamidite in the presence of diisopropyl ammonium tetrazolide as activator in anhydrous CH_2Cl_2 to afford **9** in 50% yield (Scheme 1). The obtained phosphoramidite **9** was incorporated into oligonucleotides by a standard phosphoramidite protocol on an automated DNA synthesizer. However, an extended coupling time (15 min) was used for the modified amidite in the oligonucleotide. All modified oligodeoxynucleotides (ODNs) were purified by reversed-phase HPLC, and confirmed by MALDI-TOF-MS analysis as reported in Section 7. The purity of the final sequences was determined by ion-exchange HPLC (IE-HPLC) to be more than 95%.

3. Thermal stability studies

The thermal stability of parallel triplexes and TWJ with bulge insertion of the intercalating monomer **M** was evaluated by thermal denaturation experiments using the UV melting method. The melting temperatures (T_m, °C) were determined as the maximum of the first derivative of melting curves.

TFO's thermal stability was studied with the wavelength λ = 260 nm at pH 5.0, 6.0 and 7.2. An excess of the pyrimidine to the purine strand ratio (1.5:1 mM) in the duplex was used to avoid a disturbing melting of the parallel duplex at pH 5.0 and 6.0. The triplex from the TFO **ON2** and the duplex **D1** shows high thermal stability at pH 6.0 and pH 7.2 when compared with the wild type **ON1** (Table 1). Because of overlapping triplex and duplex meltings

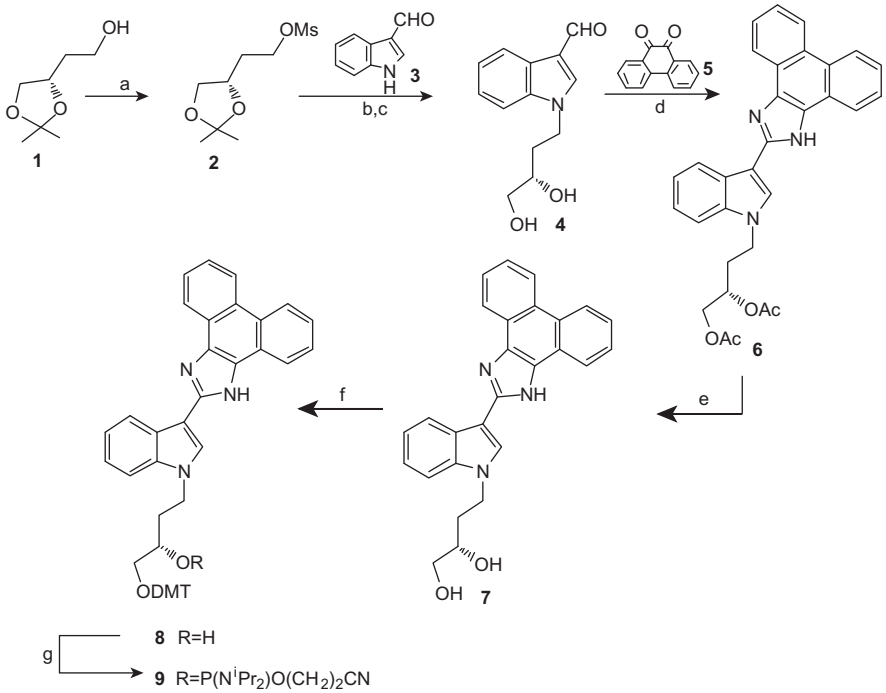

Scheme 1. Reagents and conditions: (a) MsCl, Et_3N, CH_2Cl_2, 0 °C, 2 h; (b) NaH, DMF, Et_3N, 55–60 °C, 72 h; (c) 1 N HCl, DMF, rt, 2 h; (d) CH_3COONH_4, CH_3COOH glacial, 90 °C, 72 h; (e) NH_3/MeOH, rt, 72 h; (f) DMTCl, pyridine, Et_3N rt, 72 h; (g) *N,N′*-diisopropylammonium tetrazolide, 2-cyanoethyl *N,N,N′,N′*-tetraisopropylphosphordiamidite, rt, 48 h.

at pH 5.0, the stability of the modified and wild type triplexes were also measured at $\lambda = 373$ nm where the intercalator has a UV absorption. When comparing the thermal melting with the previously published data[37] for the phenoxy comprising intercalator **X** (**ON3**) and the naphthoxy comprising **Y** (**ON4**) as shown in Table 1, we found a lower thermal stability of the newly modified indole comprising **M** TFO even though a more favorable geometry was anticipated to avoid sterical clashes. This is best seen at pH 6 where the observed triplex stability was $\Delta T_m = 6.5$ °C for the intercalator **M** compared to $\Delta T_m = 18$ °C for the intercalator **X** and $\Delta T_m = 12$ °C for **Y**. The lower stability of the indole interalator system may be explained by a shortening of the intercalator compared to the naphthoxy system which may be inserted deeper into the triplex without disturbing the backbone. Another interesting feature is the kinetics for the formation of the triplex. Therefore heating/annealing curves for the matched triplex **ON2/D1** were recorded at pH 5.0, 6.0 and 7.2 as shown in Fig. 2. At pH 6.0 there was found a hysteresis profile which was similar to a previously reported

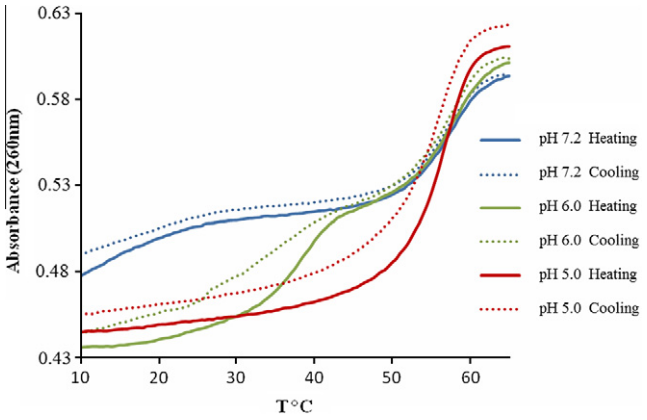

Figure 2. Melting profile of triplex melting (up and down) of **ON2**/**D1** at different pH's recorded at 260 nm versus temperature difference (1 °C/min) from 10–65 °C in 20 mM sodium cacodylate, 100 mM NaCl, 10 mM $MgCl_2$.

Table 1
T_m (°C) data for melting of triplexes evaluated from UV melting curves ($\lambda = 260$ nm)

Entry	TFO	Parallel triplex 3′-CTGCCCCTTTCTTTTTT 5′-GACGGGGAAAGAAAAAA (**D1**)		
		pH 5.0	pH 6.0	pH 7.2
ON1	5′-CCCCTTTCTTTTTT-3′	55.5[a,b]	28.5[a]	<10.0[c]
ON2	5′-CCCCTT**M**TCTTTTTT-3′	55.5[a,b]	35.0[a]	15.5[c]
ON3	5′-CCCCTT**X**TCTTTTTT-3′	59.5[c,d]	46.5[c,d]	26.0[c,d]
ON4	5′-CCCCTT**Y**TCTTTTTT-3′	55.0[c,d]	40.5[c,d]	18.5[c,d]

[a] $C = 1.5$ μM of **ON1-2**, 1.5 μM of pyrimidine strand and 1.0 μM of purine strand of dsDNA (**D1**) in 20 mM sodium cacodylate, 100 mM NaCl, 10 mM $MgCl_2$, pH 5.0 and pH 6.0.
[b] Third strand and duplex melting overlaid. T_m values confirmed at 373 nm.
[c] $C = 1.5$ μM of **ON1-3**, 1.0 μM of each strand of dsDNA (**D1**) in 20 mM sodium cacodylate, 100 mM NaCl, 10 mM $MgCl_2$, pH 5.0, pH 6.0 and pH 7.2.
[d] Data taken from Ref. 37.

hysteresis profile for a wild-type triplex[47] indicating a similarity in the kinetics for the intercalating oligonucleotide **ON2**. Due to overlapping duplex and triplex meltings at pH 5, a clear picture of the hysteresis could not be deduced which was also the case at pH 7.2 because of a low triplex melting temperature.

The sensitivity to Hoogsteen mismatches were also studied for parallel triplexes with a bulge insertion of the intercalators **M**, **X** and **Y** in the TFO at pH 6.0 (Table 2, Supplementary data, Fig. S1). **X** and **Y** was better than **M** to discriminate neighboring Hoogsteen mismatches, **ON3** (15–23.5 °C), **ON4** (15–24 °C) compared to **ON2** (10.5–16.5 °C).

Hybridisation properties of oligonucleotides **ON5–7** when targeting DNA (**ON11**) or RNA (**ON12**) forming a TWJ were evaluated in thermal stability studies at pH 7 (Table 3, Supplementary data, Fig. S2). TWJ was composed of a single stranded DNA or RNA stem-loop sequence with two single stranded regions being complementary to the oligonucleotides **ON5–7**

Table 2
T_m (°C) data for melting of mismatched Hoogsteen parallel triplexes evaluated from UV melting curves (λ = 260 nm) at pH 6.0

Entry	TFO	**D1**, **K**. **L** = T. A	**D2**, **K**. **L** = A. T	**D3**, **K**. **L** = C. G	**D4**, **K**. **L** = G. C
Sequence 3′	CTGCCCCTT***K***CTTTTTT				
	5′-GACGGGGAA***L***GAAAAAA				
ON1	5′-CCCCTTTCTTTTTT-3′	28.5[a]	<10.0[a]	<10.0[a]	<10.0[a]
ON2	5′-CCCCTT**M**TCTTTTTT-3′	35.0[a]	18.5[a]	19.0[a]	24.5[a]
ON3	5′-CCCCTT**X**TCTTTTTT-3′	46.5[b,c]	23.0[b,c]	29.5[b,c]	31.5[b,c]
ON4	5′-CCCCTT**Y**TCTTTTTT-3′	40.5[b,c]	16.5[b,c]	21.0[b,c]	25.5[b,c]

[a] C = 1.5 μM of **ON1-2**, 1.5 μM of pyrimidine strand and 1.0 μM of purine strand of dsDNA (**D1**) in 20 mM sodium cacodylate, 100 mM NaCl, 10 mM $MgCl_2$, pH 6.0.
[b] C = 1.5 μM of **ON1-3**, 1.0 μM of each strand of dsDNA (**D1**) in 20 mM sodium cacodylate, 100 mM NaCl, 10 mM $MgCl_2$, pH 6.0.
[c] Data taken from Ref. 37

Table 3
T_m (°C) data[a] for melting of DNA/RNA three-way junctions[b] evaluated from UV melting curves (λ = 260 nm) at pH 7.0

Entry		**DNA (ON11)**	**RNA (ON12)**
		TT *T T* *G C* *C G* *G C* *C G* 3’-CGA GTG A AGAGG GT-5’	*UU* *U U* *G C* *C G* *G C* *C G* 3’-CGA GUG A AGAGG GU-5’
ON5	5’-GCT CAC T**M**T CTC CCA-3’	40.5	44.0
ON6	5’-GCT CAC T**M**TT CTC CCA-3’	37.0	45.0
ON7	5’-GCT CAC TT**M**T CTC CCA-3’	39.5	43.0
ON8	5’-GCT CAC TT CTC CCA-3’	28.0	38.5
ON9	5’-GCT CAC TTT CTC CCA-3’	26.5	39.5
ON10	5’-GCT CAC TTTT CTC CCA-3’	28.5	43.0

[a] C = 1.0 μM of each strand of DNA/RNA TWJ in 15 mM Na_2HPO_4, 100 mM NaCl, 0.1 mM EDTA, pH 7.0.
[b] Italic sequences are bases incorporated in the stem loop.

having an intercalator **M** inserted at the junction in one case and in other cases with an additional thymidine base **T** before or after the intercalator **M** (Table 3). We suppose that TWJ has two coaxially stacking arms and a third deflecting arm that can be stabilized by the intercalator as a stacking lid onto that arm at the junction site. In order to evaluate the thermal stabilities of the modified TWJ we made a comparison with wild type TWJs with none, one or two insertions of **T** corresponding to the site of insertion of **M**. For DNA (**ON11**) the temperature range of the meltings were within 2 °C when hybridised with the wild type oligos **ON8–10** whereas for the same oligos upon hybridisation to RNA (**ON12**), the stability increased with the number of **T** insertions with ΔT_m = 4.5 °C when **ON10** is compared with **ON8**. For insertion of **M**, only, **ON5** resulted in an increase of more than 10 °C upon hybridisation to DNA (**ON11**) when compared to the wild type oligos (Table 3). Additional insertion of **T** (**ON6** and **ON7**) resulted in a slightly lower increase in the melting temperature. On the other hand, when the oligos with insertion of **M** were targeting RNA (**ON12**) no substantial increase in melting temperature could be obtained when compared to the wild type oligo with two **T** insertions.

The oligos **ON5** and **ON8** were used to confirm targeting on both sides of the hairpins DNA (**ON11**) and RNA (**ON12**). The sensitivity to two mismatches in one or the other arm was studied for this purpose (Table 4). For example, the hairpin from **ON13** and **ON5** is destabilized by 16.5 °C compared to the corresponding hairpin from **ON11** and **ON5**. A similar result was found for the **ON13/ON8** hairpin when compared to the wild type **ON11/ON8** hairpin (ΔT_m = −14.5 °C). Similar results were obtained for mismatches to the other side of the hairpin (Table 4). Also in case of DNA/RNA TWJ, binding to both sides of the hairpin could be proven in the same manner. The heating/annealing profile was also studied for **ON5/ON11** (Supplementary data, Fig. S3) which shows a rapid rehybridisation of the DNA-TWJ.

Table 4
T_m (°C) data[a] for melting of mismatched DNA/RNA three-way junctions[b] evaluated from UV melting curves (λ = 260 nm) at pH 7.0

Entry		5′-GCT CAC T**M**T CTC CCA-3′ (**ON5**)	5′-GCT CAC TT CTC CCA-3′ (**ON8**)
DNA	3′-CGA GTG *ACG CGT TTT CGC GAG* AGG GT-5′ (**ON11**)	40.5	28.0
	3′-CGA GTG *ACG CGT TTT CGC GAG* A<u>TT</u> GT-5′ (**ON13**)	24.0	13.5
	3′-CG<u>T T</u>TG *ACG CGT TTT CGC GAG* AGG GT-5′ (**ON14**)	18.0	<10.0
RNA	3′-CGA GUG *ACG CGU UUU CGC GAG* AGG GU-5′ (**ON12**)	44.0	38.5
	3′-CGA GUG *ACG CGU UUU CGC GAG* A<u>UU</u> GU-5′ (**ON15**)	23.0	12.5
	3′-CG<u>U U</u>UG *ACG CGU UUU CGC GAG* AGG GU-5′ (**ON16**)	21.0	17.0

[a] C = 1.0 μM of each strand of DNA/RNA TWJ in 15 mM Na_2HPO_4, 100 mM NaCl, 0.1 mM EDTA, pH 7.0.
[b] Italic sequences are bases incorporated in the stem loop, underlined bases are mismatched ones.

4. Fluorescence properties

The insertion of the intercalator **M** into oligonucleotides showed a characteristic fluorescence spectrum. The fluorescence measurements on matched and mismatched triplexes were performed with **ON2** as the TFO whereas for TWJ the targeting oligonucleotide **ON5** was used. In both cases fluorescence of single stranded oligonucleotides were also measured. In all cases, the spectra were recorded from 340 to 600 nm at 10 °C in the same buffer solutions as used for T_m studies.

The spectra of triplexes were measured upon excitation at 350 nm using 1.0 μM purine strand and 1.5 μM of both the pyrimidine strands at pH 6.0. The fluorescence intensity was stronger for the fully matched triplex **ON2/D1** compared to the single stranded **ON2**. The emission intensities of the neighboring Hoogsteen mismatches **ON2/D2** and **ON2/D4** were slightly lower and slightly higher, respectively, than for the matched **ON2/D1** whereas the emission intensity of **ON2/D3** due to G/T Hoogsteen mismatch was considerably lower, but not lower than for the single strand **ON2** (Fig. 3a). TWJ fluorescence spectra were obtained upon excitation at 330 nm, using a 1.0 μM concentration of both the hairpin strand and the modified oligonucleotide **ON5** at pH 7.0. When hybridised to DNA hairpin **ON11** or to RNA hairpin **ON12** the fully matched TWJ using the modified strand **ON5** showed the highest intensity in both cases compared to the single strand **ON5** (Fig. 3b and c).

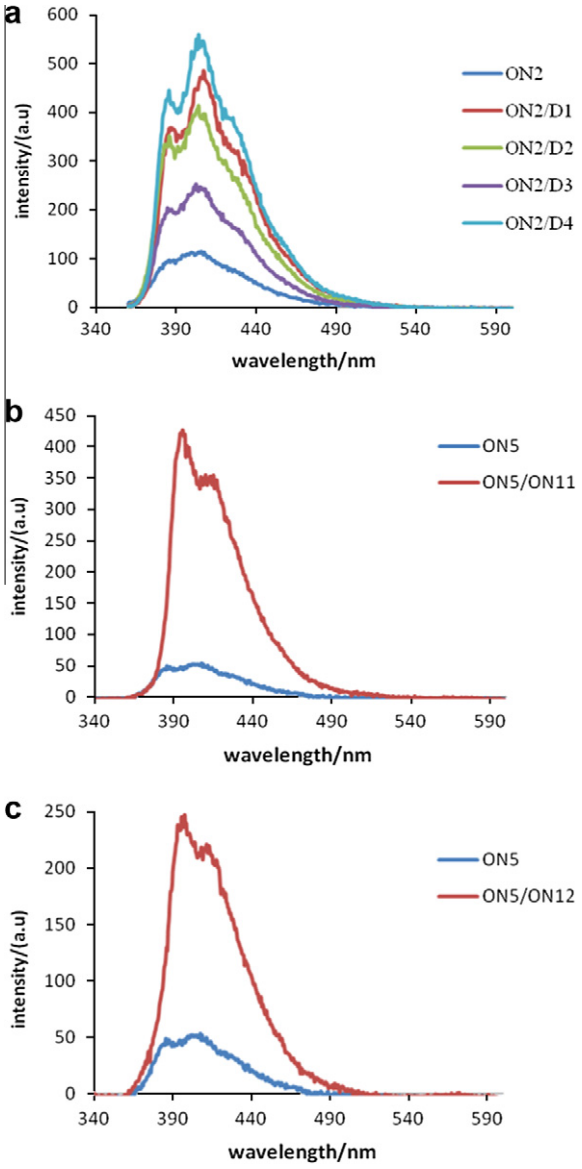

Figure 3. Fluorescence emission spectra of (a) **ON2** comprising monomer **M** upon excitation at 350 nm and pH 6.0 forming parallel triplex and mismatched triplexes. (b) **ON5** comprising monomer **M** upon excitation at 330 nm and pH 6.0 forming DNA TWJ. (c) **ON5** comprising monomer **M** upon excitation at 330 nm and pH 6.0 forming RNA TWJ.

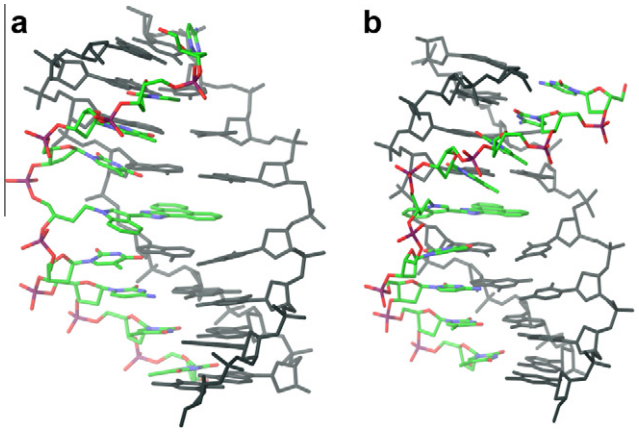

Figure 4. Representative low-energy conformations of a triplex containing bulged insertion of **M** produced by AMBER* calculations of the stacking showing phenanthroimidazole between the bases of dsDNA (a) forward fused benzene moiety, (b) backward fused benzene moiety.

5. Molecular modeling

In order to understand the intercalating properties of the new monomer **M** stabilizing the triplex, we decided to examine it via molecular modeling studies. An AMBER* force field in Macro Model 9.1, molecular modeling was used to generate representative low-energy structures of a truncated 8mer triplex with the bulge insertion of the monomer **M** into the middle of the triplex. As it can be seen from Figure 4a and b the positioning of the phenanthroimidazole moiety in the Watson–Crick duplex is adding to the triplex stability via π–π interaction. The presence of indolyl moiety positioned between nucleobases of the TFO make large extent of twisting forcing the fused benzene ring out of plane by sterical interaction between protons on the indole-moiety and on the imidazole-moiety. Twisting the indolyl moiety of intercalator **M** around the single bond resulted in conformations with almost identical intercalating properties in the triplex and no optimal conformation could be assigned. Figure 4a and b show these two types of conformations in which have low stackings between indolyl moiety and up and down nucleobases. The nucleobases of the TFO are forced to twist out of plane weakening the stacking interactions and this could explain the lower thermal stability than expected. The modeling supports the thermal stability measurements which showed a decrease in triplex stability using intercalator **M** in comparison with previously prepared intercalators **X** and **Y**, clearly demonstrating the importance of optimal π–π-stacking interactions.[48]

6. Conclusion

In this study, we have synthesized new intercalating nucleic acid monomers **M**, and incorporated it into oligonucleotides giving good yields using normal oligonucleotide synthesis procedures. Thermal melting studies showed that this intercalator was able

to stabilize Hoogsteen-type triplexes with good discrimination of mismatch strands compared to wild type triplexes. However, DNA-strands containing intercalators **X** and **Y** show higher thermal triplex stability than DNA-strands containing intercalator **M**. The intercalator **M** increased thermal stability of DNA TWJ-type with good discrimination of mismatch strands compared to wild type TWJ. In case of RNA TWJ-type, the monomer **M** was unable to contribute with any substantial.

7. Experimental

7.1. General

NMR spectra were recorded on a Bruker 400 MHz spectrometer at 400 MHz for ^{1}H, 101 MHz for ^{13}C, and 162 MHz for ^{31}P with TMS as an internal standard for ^{1}H NMR. Chemical shifts are reported in ppm, relative to solvents peaks ($CDCl_3$: 7.26 ppm for ^{1}H and 77.0 ppm for ^{13}C; DMSO-d_6: 2.50 ppm for ^{1}H and 39.5 ppm for ^{13}C; 85% aq H_3PO_4 as an external standard: 0.00 ppm for ^{31}P NMR). Electrospray ionization high resolution mass spectra (ESI-HRMS) were performed on PE SCIEX API Q-Star Pulsar Mass Spectrometer. For accurate ion mass determinations, the (MH^+) or (MNa^+) ion was peak matched by calibration with NaI. Melting points were determined on a Büchi melting point apparatus and are not corrected. An IR spectrum was run on Perkin Elmer 1720 Fourier Transform Infrared Spectrophotometer. DCM was always used freshly distilled and solvents used for column chromatography of final phosphoroamidite were distilled prior to use, others are used as received. Reagents were used as purchased. Silica gel (0.040–0.063 mm) used for column chromatography and analytical silica gel TLC plates 60 F254 precoated aluminium plates were purchased from Merck. TLC spots of DMT containing compounds was visualized as orange or dark spots when treated with 5% ethanolic H_2SO_4 solution.

7.1.1. (*S*)-1-(3,4-Dihydroxybutyl)-1*H*-indole-3-carbaldehyde (4)

To a stirred mixture of (*S*)-2,2-dimethyl-1,3-dioxolan-4-yl ethanol **1** (1.65 g, 11.3 mmol) and methanesulfonyl chloride (MsCl) (1.81 g, 15.8 mmol) in dichloromethane (CH_2Cl_2) (20 ml) was added dropwise triethylamine (Et_3N) (1.60 g, 15.8 mmol) at ice-bath temperature. After 2 h, the reaction mixture was partitioned between CH_2Cl_2 and water. The organic layer was washed with brine, dried ($MgSO_4$), and concentrated in vacuo to give the methanesulfonate **2** (2.5 g) as a colorless oil. This material was used immediately without further purification.

To a suspension of NaH (60% in mineral oil, 506 mg, 14 mmol) in DMF (10 ml) and Et_3N (3 ml) a solution of indole-3-carboxaldehyde **3** (1.00 g, 7 mmol) in dry DMF (10 ml) was added dropwise under argon. The reaction mixture was stirred for 1 h before a solution of the above prepared methanesulfonate (**2**) (2.35 g, 10.5 mmol) in DMF (10 ml) was added. The resulting mixture was stirred for 72 h at 55-60 °C. The reaction mixture was cooled to room temperature. 1 M HCl was then added and the mixture was stirred for 2 h. The mixture was diluted with EtOAc and extracted with satd aq Na_2CO_3 and satd aq NH_4Cl. The organic layer was dried ($MgSO_4$), and concentrated in vacuo. The residue was purified by column chromatography [SiO_2, DCM/EtOAc = 10:90 (v/v)] to give **4** (0.79 g, 49%) as a yellow solid; R_f 0.1 (1:9 EtOAc/Cyclohexane); mp 98–100 °C. ^{1}H NMR (DMSO) δ: 1.74 (m, 1H, C*H*HCH$_2$N), 2.04 (m, 1H, CH*H*CH$_2$N), 3.18–3.30 (m, 1H, CH*H*OH), 3.29–3.49 (m, 2H, C*H*OH, C*H*HOH), 4.27-4.48 (m, 2H, CH$_2$N), 4.57 (t, J = 5.5 Hz, 1H, CH$_2$O*H*), 4.81 (d, J = 4.9 Hz, 1H, CHO*H*), 7.26 (t, J = 7.4 Hz, 1H, indole), 7.32 (t, J = 7.6 Hz, 1H, indole), 7.63 (d, J = 8.1 Hz, 1H, indole), 8.12 (d, J = 7.8 Hz, 1H, indole), 8.30 (s, 1H, 2-H indole), 9.92 (s, 1H, CHO).^{13}C NMR (DMSO) δ: 33.48 (*C*H$_2$CH$_2$N), 43.26 (CH$_2$*C*H$_2$N), 65.66 (CH$_2$OH), 68.28 (CHOH), 110.95, 116.95, 120.95, 122.32, 123.39, 124.63, 136.90, 140.74 (indole), 184.35 (CHO). HRMS (ESI) m/z Calcd for $C_{13}H_{15}NO_3Na^+$ (MNa^+) 256.11. Found: 256.105. Anal. Calcd for $C_{13}H_{15}NO_3{\cdot}0.25\ H_2O$: C, 65.67; H, 6.57; N, 5.89. Found: C, 66.10; H, 6.38; N, 5.84.

7.1.2. (*S*)-4-(3-(1*H*-Phenanthro[9,10-*d*]imidazol-2-yl)-1*H*-indol-1-yl)butane-1,2-diyl diacetate (6)

Phenanthrene-9,10-dione **5** (0.208 g, 1 mmol) and ammonium acetate (1.27 g, 16.5 mmol) were dissolved in hot glacial acetic acid (10 ml). While the mixture was stirred, a solution of (*S*)-1-(3,4-dihydroxybutyl)-1*H*-indole-3-carbaldehyde (**4**, 0.233 g, 1 mmol) in (15 ml) of glacial acetic acid was added dropwise. The mixture was heated at 90 °C for 72 h and was then poured into water (200 ml). The mixture was neutralized with aq ammonia to pH 7 and cooled to room temperature. The precipitate was filtered off and washed with large portions of water. The residue was purified by silica gel column chromatography [SiO_2, EtOAc/Cyclohexane = 1:99, (v/v)] to give **6** (0.39 g, 76%) as a faint yellow solid; R_f 0.7 (1:99 EtOAc/Cyclohexane); mp 88–90 °C. ^{1}H NMR (DMSO) δ: 2.00 (s, 3H, CH$_3$), 2.01 (s, 3H, CH$_3$), 2.22 (m, 2H, C*H*$_2$CH$_2$N), 4.11 (dd, J = 12.0 and 5.8 Hz, 1H, CH*H*N), 4.26 (dd, J = 12.0 and 3.2 Hz, 1H, C*H*HN), 4.42 (t, J = 7.1 Hz, 2H, C*H*$_2$OCOCH$_3$), 5.07 (m, 1H, C*H*O-COCH$_3$), 7.22-7.38 (m, 2H, ArH), 7.62 (m, 3H, ArH), 7.73 (t, J = 7.1 Hz, 1H, ArH), 7.77 (t, J = 7.1 Hz, 1H, ArH), 8.23 (s, 1H, indole), 8.45 (d, J = 8.0 Hz, 1H, ArH), 8.68 (d, J = 7.9 Hz, 1H, ArH), 8.73 (dd, J = 6.0 and 2.8 Hz, 1H, ArH), 8.85 (d, J = 8.3 Hz, 1H, ArH), 8.88 (d, J = 8.4 Hz, 1H, ArH), 13.12 (s, 1H, NH). ^{13}C NMR (DMSO) δ: 20.50 (CH$_3$), 20.72 (CH$_3$), 30.71 (*C*H$_2$CH$_2$N), 42.41 (CH$_2$*C*H$_2$N), 64.23 (CH$_2$OH), 69.22 (CHOH), 106.64, 110.21, 120.46, 121.52, 121.86, 121.99, 122.30, 122.39, 123.63, 124.07, 124.68, 125.70, 126.09, 126.94, 126.99, 127.17, 127.80, 136.25, 136.85, 146.87 (Ar), 170.05 (C=O), 170.16 (C=O). IR (cm^{-1}) 3419 (b, NH); 2929 (s, CH$_3$); 1740 (s, C=O); 1619 (s, C=N). HRMS (ESI) m/z Calcd for $C_{31}H_{28}N_3O_4^+$ (MH^+) 506.2075. Found: 506.2061.

7.1.3. (S)-4-(3-(1*H*-Phenanthro[9,10-*d*]imidazol-2-yl)-1*H*-indol-1-yl)butane-1,2-diol (7)

Diacetylated compound **6** (168 mg, 0.33 mmol) was dissolved in saturated NH_3/MeOH (20 ml), and the resulting solution was stirred at room temperature for 72 h. The solvent was removed under reduced pressure. The residue was suspended in dichloromethane and filtration afforded 110 mg (78%) of **7** as a yellow solid in a state of purity; R_f 0.2 (1:15 CH$_3$OH/DCM); mp: 267–268 °C. ^{1}H NMR (DMSO) δ: 1.74-2.19 (m, 2H, C*H*$_2$CH$_2$N), 3.31 (dt, J = 11.0 and 5.7 Hz, 1H, CH*H*OH), 3.41 (m, 2H, C*H*HOH+ C*H*OH), 4.50-4.39 (m, 2H, CH$_2$N), 4.69 (t, J = 5.5 Hz, 1H, CH$_2$O*H*), 4.90 (d, J = 5.1 Hz, 1H, CHO*H*), 7.36–7.28 (m, 2H, ArH), 7.67-7.59 (m, 3H, ArH), 7.76 (t, J = 7.5 Hz, 2H, ArH), 8.27 (s, 1H, 2-H indole), 8.45 (d, J = 7.9 Hz, 1H, ArH), 8.69 (d, J = 7.7 Hz, 1H, ArH), 8.73 (dt, J = 6.6 and 2.7 Hz, 1H, ArH), 8.84 (d, J = 8.4 Hz, 1H, ArH), 8.87 (d, J = 8.4 Hz, 1H, ArH), 13.18 (s, 1H, NH). ^{13}C NMR (DMSO) δ: 33.91 (*C*H$_2$CH$_2$N), 42.87 (CH$_2$*C*H$_2$N), 65.78 (CH$_2$OH), 68.47 (CHOH), 106.15, 110.29, 120.36, 121.48, 121.91, 122.30, 123.61, 124.04, 124.69, 125.67, 126.05, 126.95, 127.15, 128.20, 136.30, 136.83, 147.05 (Ar). HRMS (ESI) m/z Calcd for $C_{27}H_{24}N_3O_2^+$ (MH^+) 422.1863. Found: 422.1855. Anal. Calcd for $C_{27}H_{23}N_3O_2{\cdot}0.5\ H_2O$: C, 75.33; H, 5.62; N, 9.76. Found: C, 75.51; H, 5.35; N, 9.62.

7.1.4. (*S*)-4-(3-(1*H*-Phenanthro[9,10-*d*]imidazol-2-yl)-1*H*-indol-1-yl)-1-(bis(4-methoxyphenyl)(phenyl)methoxy)butan-2-ol (8)

(*S*)-4-(3-(1*H*-Phenanthro[9,10-*d*]imidazol-2-yl)-1*H*-indol-1-yl)-butane-1,2-diol (**7**, 150 mg, 0.36 mmol) was coevaporated with anhydrous pyridine (2×20 ml) and dissolved in anhydrous pyridine (20 ml) and Et_3N (2.5 ml). 4,4′-Dimethoxytrityl chloride

(160 mg, 1.3 mmol) was added under a nitrogen atmosphere, and the reaction mixture was stirred at room temperature for 72 h. The reaction was quenched by addition of MeOH (2 ml) followed by addition of DCM/Et_3N (1%) and washed twice with saturated aq $NaHCO_3$. The organic phases were washed with brine, dried ($MgSO_4$), filtered and evaporated under diminished pressure. The residue was coevaporated twice with toluene/EtOH 15 ml, (1:1, v/v). The residue was purified by column chromatography [SiO_2, NEt_3/CH_3OH/DCM = 1:0.5:98.5, (v/v/v)] to afford the DMT protected diol **8** as a yellow solid. (220 mg, 85%); R_f 0.75 (1:15 CH_3OH/DCM); mp: 165-166 °C. ^1H NMR ($CDCl_3$) δ: 1.84-2.12 (m, 2H, C$H_2$$CH_2$N), 2.97–3.07 (m, 2H, C$H_2$ODMT), 3.70 (s, 6H, 2×$OCH_3$), 3.75 (m, 1H, C*H*OH), 4.27–4.53 (m, 2H, CH_2N), 4.64 (s, 1H, CHO*H*), 6.72 (dd, *J* = 8.9 and 1.2 Hz, 4H, DMT), 7.09–7.27 (m, 8H, ArH), 7.28-7.31 (m, 1H, phenyl), 7.32-7.40 (m, 3H, ArH), 7.52 (s, 2H, ArH), 7.56 (s, 2H, ArH), 8.65 (d, *J* = 8.3 Hz, 2H, ArH), 8.84–8.74 (m, 2H, ArH), 8.87 (s, 2H, ArH), 13.47 (s, 1H, NH). ^{13}C NMR ($CDCl_3$) δ: 33.37 (*C*$H_2$$CH_2$N), 42.85 ($CH_2$*C*$H_2$N), 55.19 (2×$OCH_3$), 66.52 (CHOH), 67.72 ($CH_2$ODMT), 85.75 ($OCPh_3$), 106.18, 109.72, 113.01, 120.62, 122.24, 122.30, 123.31, 124.58, 126.47, 126.65, 126.92, 127.62, 127.71, 128.25, 130.07, 130.09, 130.79, 136.09, 136.34, 144.89, 147.89, 158.33 (Ar). HRMS (ESI) *m*/*z* Calcd for $C_{48}H_{42}N_3O_4^+$ (MH^+) 724.317. Found: 724.3193.

7.1.5. (*S*)-4-(3-(1*H*-Phenanthro[9,10-*d*]imidazol-2-yl)-1*H*-indol-1-yl)-1-(bis(4-methoxyphenyl)(phenyl)methoxy)butan-2-yl 2-cyanoethyl diisopropylphosphoramidite (9)

DMT-protected compound **8** (0.22 g, 0.3 mmol) was dissolved under an argon atmosphere in anhydrous CH_2Cl_2 (15 ml). *N,Ń*-Diisopropylammonium tetrazolide (115 mg, 0.68 mmol) was added, followed by dropwise addition of 2-cyanoethyl *N,N,Ń,Ń*-tetraisopropylphosphordiamidite (410 mg, 1.35 mmol) under external cooling with an ice-water bath. The reaction mixture was stirred at room temperature for 48 h before quenching with H_2O (10–20 ml). The layers were separated and the organic phase was washed with H_2O (10–20 ml). The combined water layers were extracted with CH_2Cl_2 (25 ml). The combined organic phase was dried (Na_2SO_4) and filtered, and the solvent was evaporated in vacuo. The residue was purified by column chromatography [SiO_2, NEt_3/EtOAc/cyclohexane = 1: 20:79, (v/v/v)] to afford the final product **9** as a yellow solid (140 mg, 50%); R_f 0.73 (1:4 EtOAc/cyclohexane), which was used in DNA synthesis after drying under diminished pressure. ^{13}C NMR ($CDCl_3$) δ: 21.02 (*C*H_2CN), 22.67 (CH_3), 22.82 (CH_3), 23.44 (CH_3), 24.62 (CH_3), 33.67 (*C*$H_2$$CH_2$N), 43.07 ($CH_2$*C*$H_2$N), 45.58 (N*C*H($CH_3$)$_2$), 45.63 (N*C*H($CH_3$)$_2$), 55.18 (2×$OCH_3$), 60.34 (O*C*$H_2$$CH_2$CN), 68.18 (CHOP), 69.25 (CH_2ODMT), 86.07 ($OCPh_3$), 99.96, 109.58, 113.11, 120.79, 122.46, 126.74, 127.80, 128.07, 129.11, 130.02, 135.92, 144.79, 158.45 (Ar). ^{31}P NMR ($CDCl_3$) δ: 148.06, 148.69 in a 1:3 ratio. HRMS (ESI) *m*/*z* Calcd for $C_{57}H_{58}N_5O_5PNa^+$ (MNa^+) 946.4068. Found: 946.4062.

7.2. Oligonucleotide synthesis, purification, and melting temperature determination

DMT-off oligodeoxynucleotides were carried out at 0.2 μmol scales on 500 Å CPG supports with an Expedite™ Nucleic Acid Synthesis System Model 8909 from Applied Biosystems with 1H-tetrazole as an activator for coupling reaction. The amidite **9** was dissolved in dry DCM and inserted into the growing oligonucleotides chain using an extended coupling time (15 min). DMT-off oligonucleotides bound to CPG supports were treated with aqueous ammonia (32%, 1 ml) at room temperature for 20 min and then at 55 °C overnight. Purification of DMT-off ONs was accomplished by reversed-phase semipreparative HPLC on a Waters Xterra MS C18 5 μm, 7.8×150 mm column with a Waters Xterra MS C18 5 μm, 7.8×10 mm Chromatography System (Buffer A [0.05 M triethylammonium acetate (pH 7.4)] and Buffer B (75% MeCN/25% Buffer A)). Flow 2.5 ml/min. Gradients: 2 min 100% A, linear gradient to 70% B in 38 min, linear gradient to 100% B in 7 min and then 100% A in 10 min). 80% Acetic acid were added to ODNs over 20 min, afterwards 100 μL double filtered water, aqueous AcONa (3 M, 15 μL) and aqueous Sodium perchlorate (5 M, 15 μL) were then added and the ONs were precipitated from pure acetone. All modified ODNs were confirmed by MALDI-TOF analysis on a Ultraflex II TOF/TOF system from Bruker (a MALDI-LIFT system) with HPA-matrix (10 mg 3-hydroxypicolinic acid, in 50 mM ammoniumcitrate/70% acetonitril) matrix. ODN Found *m*/*z* (Calculated *m*/*z*): **ON2** 4609.0 (4603.8), **ON5** 4609.9 (4616.8), **ON6** 4916.9 (4921.0) and **ON7** 4925.6 (4921.0). The purity of the final TFOs was found to be over 95%, checked by ion-exchange chromatography using La-Chrom system from Merck Hitachi on Dionex DNAPac Pa-100, 4 × 250 mm Analytical column. Melting temperature measurements were performed on a Perkin–Elmer UV–Vis spectrometer Lambda 35 fitted with a PTP-6 temperature programmer. The triplexes were formed by first mixing the two strands of the Watson–Crick duplex, at a concentration of 1.0 or 1.5 μM according to the method mentioned above in the Thermal stability studies part, followed by addition of the third (TFO) strand at a concentration of 1.5 μM in a buffer consisting of sodium cacodylate (20 mM), NaCl (100 mM), and $MgCl_2$ (10 mM) at pH 5.0, pH 6.0 or 7.2. TWJs were formed by mixing the two strands each at a concentration of 1.0 μM in sodium phosphate buffer (15 mM) containing NaCl (100 mM) and EDTA (0.1 mM) at pH 7.0. The solutions were heated to 80 °C then cooled down to 10 °C and were then kept at this temperature for 30 min. The melting temperature (T_m, °C) was determined as the maximum of the first derivative plots of the melting curves obtained by absorbance at 260 nm against increasing temperature (1.0 °C /min). If needed experiments were also done at 373 nm.

7.3. Fluorescence measurements

The fluorescence measurements were measured on a Perkin–Elmer LS-55 luminescence spectrometer fitted with a julabo F25 temperature controller set at 10 °C in the buffer 20 mM sodium cacodylate, 100 mM NaCl, and 10 mM $MgCl_2$ at pH 6.0 for triplex formation using the same solution used for T_m measurements, setting excitation and emission slits to 4 and 2.5 nm respectively and upon excitation at 350 nm. For TWJs formation, the fluorescence instrument was set at 10 °C in the buffer 15 mM sodium phosphate, 100 mM NaCl and 0.1 mM EDTA at pH 7.0, upon excitation at 330 nm, using a 1.0 μM concentration of both hairpin strands and modified oligonucleotide **ON5** and setting excitation and emission slits were set to 4 and 0.0 nm respectively. The 0.0 nm slit is not completely closed and allowed sufficient light to pass for the measurement.

7.4. Molecular modeling

Molecular modeling was performed with Macro Model v9.1 from Schrödinger. All calculations were conducted with AMBER* force field and the GB/SA water model. The dynamic simulations were preformed with stochastic dynamics, a SHAKE algorithm to constrain bonds to hydrogen, time step of 1.5 fs and simulation temperature of 300 K. Simulation for 0.5 ns with an equilibration time of 150 ps generated 250 structures, which all were minimized using the PRCG method with convergence threshold of 0.05 kJ/mol. The minimized structures were examined with Xcluster from Schrödinger, and representative low-energy structures were selected. The starting structures were generated with Insight II

v97.2 from MSI, followed by incorporation of the modified nucleotide.

Acknowledgments

This work was supported by the Nucleic Acid Center, which is funded by The Danish National Research Foundation for studies on nucleic acid chemical biology; also a part of the funding was supported by the Cultural Affairs & Missions Sector, Ministry of Higher Education, Egypt.

Supplementary data

Supplementary data (thermal denaturation first derivative plots of matched and mismatched triplex melting (**ON1/D1-4** and **ON2/D1-4**) in addition to DNA/RNA TWJs melting (**ON5/ON11-15**) and **ON8/ON11-15**); DNA TWJ heating/annealing profile for **ON5/ON11;** UV absorption spectrum of **M** diol (Supplementary data, Fig. S4) and ^{1}H NMR of prepared compounds) associated with this article can be found, in the online version, at doi:10.1016/j.bmc.2011.11.013.

References and notes

1. Felsenfeld, G.; Rich, A. *Biochim. Biophys. Acta* **1957**, *26*, 457.
2. Thenmalarchelvi, R.; Yathindra, N. *Nucleic Acids Res.* **2005**, *33*, 43.
3. Goni, J. R.; De La Cruz, X.; Orozco, M. *Nucleic Acids Res.* **2004**, *32*, 354.
4. Sargent, R. G.; Kim, K. *Dieter C.; Gruenert, D. C. Oligonucleotides* **2011**, *21*, 55.
5. Htun, H.; Dahlberg, J. E. *Science* **1989**, *243*, 1571.
6. Jain, A. K.; Bhattacharya, S. *Bioconjugate Chem.* **2010**, *21*, 1389.
7. Duca, M.; Vekhoff, P.; Oussedik, K.; Halby, L.; Arimondo, P. B. *Nucleic Acids Res.* **2008**, *36*, 5123.
8. Arimondo, P. B.; Boutorine, A.; Baldeyrou, B.; Bailly, C.; Kuwahara, M.; Hecht, S. M.; Sun, J. S.; Garestier, T.; Helene, C. *J. Biol. Chem.* **2002**, *277*, 3132.
9. Panakanti, R.; Pratap, A.; Yang, N.; Jackson, J. S.; Mahato, R. I. *Biochem. Pharmacol.* **2010**, *80*, 1718.
10. Sedelnikova, O. A.; Karamychev, V. N.; Panyutin, I. G.; Neumann, R. D. *Antisense Nucleic Acid Drug Dev.* **2002**, *12*, 43.
11. Besch, R.; Marschall, C.; Schuh, T.; Giovannangeli, C.; Kammerbauer, C.; Degitz, K. *J. InVest. Dermatol.* **2004**, *122*, 1114.
12. Hahn, W. C.; Counter, C. M.; Lundberg, A. S.; Roderick, L.; Beijersbergen, R. L.; Mary, W.; Brooks, M. W.; Robert, A.; Weinberg, R. A. *Nature* **1999**, *400*, 464.
13. Samadashwily, G. M.; Mirkin, S. M. *Gene* **1994**, *149*, 127.
14. Francois, J. C.; Saison-Behmoaras, T.; Thoung, N. T.; Helene, C. *Biochemistry* **1989**, *28*, 9617.
15. Maher, L. J.; Wold, B.; Dervan, P. B. *Science* **1989**, *245*, 725.
16. Roulon, T.; Coulaud, D.; Delain, E.; Le Cam, E.; Hélène, C.; Escudé, C. *Nucleic Acids Res.* **2002**, *30*, e-12.
17. Prakash, G.; Kool, E. *J. Am. Chem. Soc.* **1992**, *114*, 523.
18. Orr-Weaver, T. L.; Szostak, J. W.; Rothstein, R. J. *Proc. Natl. Acad. Sci. U.S.A.* **1981**, *78*, 6354.
19. Guthrie, C.; Patterson, B. *Annu. ReV. Genet.* **1988**, *22*, 387.
20. (a) Wimberly, B. T.; Brodersen, D. E.; Clemons, W. M.; Morgan-Warren, R. J.; Carter, A. P.; Vonrhein, C.; Hartsch, T.; Ramakrishnan, V. *Nature* **2000**, *407*, 327; (b) Ban, N.; Nissen, P.; Hansen, J.; Moore, P. B.; Steitz, T. A. *Science* **2000**, *289*, 905.
21. Singleton, M. R.; Scaife, S.; Wigley, D. E. *Cell* **2001**, *107*, 79.
22. Hutchins, C. J.; Rathjen, P. D.; Forster, A. C.; Symons, R. H. *Nucleic Acids Res.* **1986**, *14*, 3627.
23. Pearson, C. E.; Tam, M.; Wang, Y. H.; Montgomery, S. E.; Dar, A. C.; Cleary, J. D.; Nichol, K. *Nucleic Acids Res.* **2002**, *30*, 4534.
24. La Bean, H. T.; Yan, H.; Kopatsch, J.; Liu, F. R.; Winfree, E.; Rief, J. H.; Seeman, N. C. *J. Am. Chem. Soc.* **2000**, *112*, 1848.
25. Muhuri, S.; Mimura, K.; Miyoshi, D.; Sugimoto, N. *J. Am. Chem. Soc.* **2009**, *131*, 9268.
26. Leitner, D.; Schröder, W.; Weisz, K. *Biochemistry* **2000**, *39*, 5886.
27. Fox, K. R. *Curr. Med. Chem.* **2000**, *7*, 17.
28. Brunet, E.; Corgnali, M.; Perrouault, L.; Roig, V.; Asseline, U.; Sørensen, M. D.; Babu, B. R.; Wengel, J.; Giovannangeli, C. *Nucleic Acids Res.* **2005**, *33*, 4223.
29. Olsen, A. G.; Dahl, O.; Nielsen, P. E. *Nucleosides, Nucleotides Nucleic Acids* **2003**, *22*, 1331.
30. Christensen, U. B.; Pedersen, E. B. *Nucleic Acids Res.* **2002**, *30*, 4918.
31. Natsume, T.; Ishikawa, Y.; Dedachi, K.; Tsukamoto, T.; Kurita, N. *Chem. Phys. Lett.* **2007**, *434*(1–3), 133.
32. (a) Arya, D. P.; Coffee, R. L., Jr.; Charles, I. *J. Am. Chem. Soc.* **2001**, *123*, 11093; (b) Arya, D. P. *Acc. Chem. Res.* **2011**, *44*, 134; (c) Shaw, N. N.; Arya, D. P. *Biochimie* **2008**, *90*, 1026; (d) Xue, L.; Xi, H.; Kumar, S.; Gray, D.; Davis, E.; Hamilton, P.; Skriba, M.; Arya, D. P. *Biochemistry* **2010**, *49*, 5540.
33. Johnson, H. A.; Thomas, N. R. *Bioorg. Med. Chem. Lett.* **2002**, *12*, 237.
34. Chen, C.; Song, G.; Yang, X.; Ren, J.; Qu, X. *Biochimie* **2010**, *92*, 1416.
35. (a) Filichev, V. V.; Pedersen, E. B. *J. Am. Chem. Soc.* **2005**, *127*, 14849; (b) Pandey, P. C.; Weetall, H. *Appl. Biochem. Biotechnol.* **1995**, *55*, 87.
36. Filichev, V. V.; Gaber, H.; Olsen, T. R.; Jørgensen, P. T.; Jessen, C. H.; Pedersen, E. B. *Eur. J. Org. Chem.* **2006**, *17*, 3960.
37. Osman, A. M. A.; Jørgensen, P. T.; Bomholt, N.; Pedersen, E. B. *Bioorg. Med. Chem.* **2008**, *16*, 9937.
38. Barbaric, J.; Wanninger-Weiß, C.; Wagenknecht, H. *Eur. J. Org. Chem.* **2009**, *3*, 364.
39. Bähn, S.; Imm, S.; Mevius, K.; Neubert, L.; Tillack, A.; Williams, J. M. J.; Beller, M. *Chem. Eur. J.* **2010**, *16*, 3590.
40. Kim, B. Y.; Ahn, J. B.; Lee, H. W.; Moon, K. S.; Sim, T. B.; Shin, J. S.; Ahn, S. K.; Hong, C. I. *Chem. Pharm. Bull.* **2003**, *51*, 276.
41. Zahran, M. A.; Ibrahim, A. M. *J. Chem. Sci.* **2009**, *121*, 455.
42. (a) Billes, F.; Podea, P. V.; Ziegler, I. M.; Toşa, M.; Mikosch, H.; Irimie, D. *Spectrochim. Acta, Part A* **2009**, *74*, 1031; (b) Giraud, F.; Loge, C.; Pagniez, F.; Crepin, D.; Barres, S.; Picot, C.; Le Pape, P.; Le Borgne, M. *J. Enzyme Inhibition Med. Chem.* **2009**; *24*, 1067.
43. Terasaka, T.; Kinoshita, T.; Kuno, M.; Seki, N.; Tanaka, K.; Nakanishi, I. *J. Med. Chem.* **2004**, *47*, 3730.
44. Krebs, F. C.; Spanggaard, H. *J. Org. Chem.* **2002**, *67*, 7185.
45. Mansurova, M.; Koay, M. S.; Gärtner, W. *Eur. J. Org. Chem.* **2008**, *32*, 5401.
46. Gillaizeau, I.; Lagoja, I. M.; Nolan, S. P.; Aucagne, V.; Rozenski, J.; Herdewijn, P.; Agrofoglio, L. A. *Eur. J. Org. Chem.* **2003**, *4*, 666.
47. Rougbe, M.; Faucon, B.; Mergny, J. L.; Barcelo, F.; Giovannangeli, C.; Garestier, T.; Hèléne, C. *Biochemistry* **1992**, *31*, 9269.
48. Bomholt, N.; Osman, A. M. A.; Pedersen, E. B. *Org. Biomol. Chem.* **2008**, *6*, 3714.